Computationally Guided Ligand Discovery from Compound Libraries and Discovery of a New Class of Ligands for Ni-Catalyzed Cross-Electrophile Coupling of Challenging Quinoline Halides

Sergei Tcyrulnikov,[†] Aran K. Hubbell,[†] Dylan Pedro,[†] Giselle P. Reyes,[†] Sebastien Monfette,*[†] Daniel J. Weix,*[‡] and Eric C. Hansen*[†]

†Chemical Research and Development, Pfizer Worldwide Research and Development, Eastern Point Road, Groton, Connecticut 06340, United States.

‡University of Wisconsin-Madison, Madison, Wisconsin 53706, United States

ABSTRACT: Although screening technology has heavily impacted the fields of metal catalysis and drug discovery, its application to the discovery of new catalyst classes has been limited. The diversity of on- and off-cycle pathways, combined with incomplete mechanistic understanding, means that screens of potential new ligands have thus far been guided by intuitive analysis of metal binding potential. This has resulted in the discovery of new classes of ligands, but the low hit rates have limited the use of this strategy because large screens require considerable cost and effort. Here we demonstrate a method to identify promising screening directions via simple, scalable computational and linear regression tools that leads to a substantial improvement in hit rate, enabling the use of smaller screens to find new ligands. The application of this approach to a particular example of Ni-catalyzed cross-electrophile coupling of aryl halides with alkyl halides revealed a previously overlooked trend: reactions with more electron-poor amidine ligands result in higher yield. Focused screens utilizing this trend were more successful than serendipity-based screening and led to the discovery of two new types of ligands, pyridyl oxadiazoles and pyridyl oximes. These ligands are especially effective for couplings of bromo- and chloro-quinolines and -isoquinolines, where they are now the state of the art. The simplicity of these models, with parameters derived from metal-free ligand structures, should make this approach scalable and widely accessible.

Introduction

Metal-catalyzed reactions play a critical role in modern synthetic chemistry.¹ One of the most effective methods to control the reactivity of transition-metal catalysts is modulation of the ligand environment. Due to the high complexity of real chemical systems, ligand discovery and design is often performed in a trial and error fashion (Figure 1A).².³ For the same reason, applications of computational techniques to the discovery of new ligand classes are limited (as opposed to optimization of a known ligand classes are ligands can be an iterative, slow process.^{8,9} High-throughput screening (HTS) technology can mitigate the inefficiency of the trial and error discovery approach by providing large amount of data quickly, but it can be resource intensive.¹¹¹¹¹¹

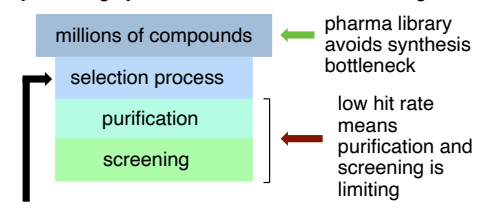
We previously reported on a new HTS-enabled ligand discovery strategy: screening of a pharmaceutical library containing a large number of densely-functionalized small molecules bearing many heteroatoms (Figure 1B). This approach provided a means to identify enabling ligand features and accelerate the discovery of new ligand core structures. Application of this strategy led to the discovery of the pyridyl amidine ligand families (PyCam) that have shown privileged reactivity for nickel-catalyzed reductive cross-electrophile coupling (XEC).¹⁵⁻¹⁷ This approach has been applied by others towards the nickel-catalyzed XEC of sterically hindered alkyl electrophiles (new imidazole nitrile ligand class, Boehringer-Ingelheim) and the Cu-catalyzed Ullman coupling of bulky coupling partners (new pyrrole alcohol ligand class, AbbVie).^{18,19} Researchers at Merck and Princeton also applied this strategy toward nickel-

catalyzed photoredox decarboxylative arylation (new phthalimide ligand/additive). Despite these successes, serendipitous discovery can be an inefficient and unreliable approach to implement. To compensate for the expected low hit rate, this strategy heavily relies upon the testing of large compound libraries. This is a time-intensive process, sometimes requiring extensive compound re-purification. Additionally, large compound libraries are not available to the majority of the synthetic community.

A. Few commercial achiral/racemic N2-ligands

N N 22 achiral/racemic how to find new /s ligands faster?

B. Pharma compound libraries can speed discovery by avoiding synthesis, but low hit rate is limiting



C. This study: increase hit rate using computationally-guided selection process

Figure 1. There are a limited number of commercial N2 ligands and new ligand discovery is a slow-process (A). The use of pharmaceutical compound libraries avoids synthesis, but the low hit-rate means purification and screening become limiting (B). This study introduces a computational guide for ligand selection (C). Ligand count from Strem catalog, accessed 12/3/2023.

Herein, we describe how the application of relatively simple correlations to refine empirical ligand selection accelerated the discovery of two new classes of ligands for nickel-catalyzed crosselectrophile coupling (Figure 1C). The new oxime ligand class is the best reported to date for the XEC of pharmaceutically relevant α haloquinoline and -isoquinoline electrophiles.

Results and Discussion

Approach. We theorized that qualitative computational evaluation of reactivity trends could be used to guide the selection of promising novel ligands without carrying out a detailed experimental or computational mechanistic investigation.²¹ Based on this proposal, we envisioned a following three-step hybrid ligand discovery approach (Figure 2):

- (A) Evaluation of a set of known ligands or utilization of existing ligand results for a reaction class of interest.
- (B) Develop simple trends from the reactions with known ligands.
- (C) Utilize these trends to further filter / prioritize potential ligands for screening.

A. Utilize Data from Known Ligands

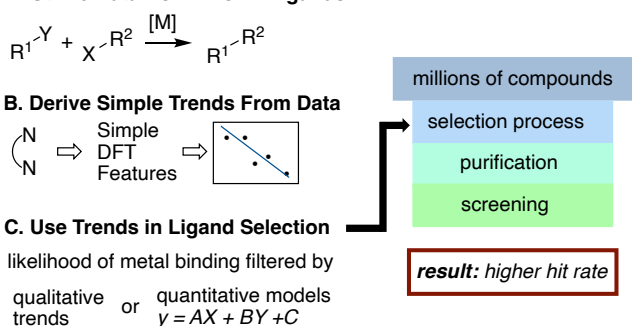


Figure 2. Computationally-guided approach for the discovery of new ligand cores among compound libraries.

Previous ligand discovery efforts have selected ligands based upon the perception of potential binding (usually from an arrangement of heteroatoms capable of bindentate binding to a metal). 15,18,19 This step may have also incorporated elements of explicit rationale, such as the selection of molecules containing a particular substructure or functionality. Our refined process introduces an additional layer of refinement in the selection of promising novel ligands by rating prospective ligands using computationally-based analysis (Figure 2C). The proposed calculations consist of rapid assesment of known experimental data and can quickly reveal ligand features that are critical for the success of a given reaction. The experimental data required to generate quantitative reactivity trends is often accessible from published ligand optimization tables. Alternatively, a preliminary, 'gauge' screen can be used to collect the desired data.²² After desired calculations are performed, ligands can be parametrized²³ with respect to computationally identified interactions. Such parametrization can be viewed as a special case of more general, nonbiased parametrization.^{24,25} By reducing the dimensionality of the parameter space, this approach provides the opportunity for a rapid analysis of potential correlations without the need for a large computational parameter set. The resulting qualitative trends

relating efficiency of the ligand to a small set of parameters can then be used to prioritize ligand selection for future experiments.

This approach acknowledges the necessity of experimental discovery techniques and utilizes computations as a supporting technique to increase the success rate and minimize experimental cost. Critically, within the described approach, computational insight is not the sole discovery tool. This deprioritizes the importance of explicit computational prediction of new reactivity in complex chemical systems.

Selection of a model system. Nickel-catalyzed XEC has become an important synthetic tool in the past decade. ^{26–35} Despite these advances, the existing set of validated ligands fail to effectively couple several important heteroaryl cores, providing no or synthetically unusable yields.³⁶ Therefore, we decided to use our proposed approach to identify new ligand classes for $C(sp^2)-C(sp^3)$ XEC reactions. We began by reevaluating the experimental dataset generated in our previous studies on ligand discovery in nickelcatalyzed XEC.15 As shown in Figure 3, various PyCam ligands are significantly more efficient than typical bpy-based ligands in the coupling of ethyl 3-bromobenzoate and 1-bromo-3-phenyl propane. This data was used to obtain parametric trends and guide the selection ligand in additional ligand discovery efforts. There was one additional advantage to this gauge data set: this challenging coupling was different from our previous ligand discovery efforts, offering an increased opportunity to find new ligands.³⁷

CO₂Et Br Ph CO₂Et
$$\frac{5 \text{ mol}\% \text{ NiCl}_2(\text{dme}), 5 \text{ mol}\% \text{ L}}{25 \text{ mol}\% \text{ Nal, 2 eqiuv Zn, 0.1 equiv TFA, DMA, 60 °C, 24h}}$$
Ligands:

$$R^{1} \frac{1}{N} \frac{18 \text{ examples}}{N} \frac{18 \text{ examples}}{N} \frac{18 \text{ examples}}{N} \frac{1}{N} \frac{1}{N$$

Figure 3. Model cross-electrophile coupling reaction used for mechanistic analysis. Average assay yields (AY, %) are provided for each class of ligand. 15

Identification of reactivity trends. Comparative analysis of key transition states commonly proposed for cross-electrophile couplings^{38,39} — radical addition to Ni(II) and reductive elimination from Ni(III)—revealed significant structural similarities between bpy and PyCam-ligated Ni systems (see Supporting Information). This led to us to propose that a difference in reactivity between PyCam and bpy-based systems may be largely due to electronic effects rather than changes in transition state geometries.

Based on this hypothesis, we parameterized PyCam ligands using atomic charges of the coordinating nitrogen atoms (Figure 4). For this analysis we considered 'free', uncoordinated ligands in their lowest energy conformations. For the pyridyl and amidine nitrogen atoms we computed Mulliken, Atomic Polar Tensor (APT), Merz-Singh-Kollman electrostatic potential (MK ESP), Hirshfeld, CM5 and natural population (NPA) atomic charges. Visual inspection of the resulting trends between charges and assay yields (AY) indicated that Mulliken charges were an effective metric of catalyst efficiency (Figure 4 shows performance of model). For a selection of PyCam

ligands we identified a bilinear regression using Mulliken charges on non-pyridine and pyridine fragments (see Figure 4, SI for details):

$$AY = 78.66 N_{Non-Py} + 296.20 N_{Py} + 79.20$$
 (1)

This trend suggests that more electron-poor amidine ligands (as indicated by a Mulliken charge) perform better in the reaction. Although we recognize that this trend may not be general and Mulliken charges have limitations, the development of this model required only a fraction of the time required for more rigorus computational approaches.

Figure 4. List of the ligands used as a training set (T) and a performance of the bilinear Mulliken charge model (eq 1) identified using this set.

Application of the identified trend. To test our model, we compared a series of ligand sets that were evaluated in the coupling of interest. To provide a relevant control, we first constructed a set of 32 small molecules (set A, not shown, see SI) that were used in our original work on PyCam ligands. Selected according to their commercial availability and perceived structural similarity to the better-performing PyCam family of ligands. We emperically biased our ligand selection towards more electron-poor systems, as suggested by the model (eq 1). In order to interrogate the quality of our model (eq 1), we divided set B into two equally sized subsets based on each ligand's predicted AY: ligands with high (subset D) and low (subset C) predicted yield (Figure 5). Set D is a final product of a proposed combined model-driven empirical ligand search.

The results of evaluating each ligand in the model reaction are presented as assay yield distributions by ligand set (Figure 6). One of the observations that can be made from the analysis of presented distributions is a relative position of both mean and median yields for described ligand sets. Despite containing one high-yielding example, the low median and mean assay yield provided by set A

demonstrates the low hit-rate (generally a "hit" is understood as a case of any desirable experimental outcome, in our particular case — a yield above some threshold) of empirical ligand selection. In fact,

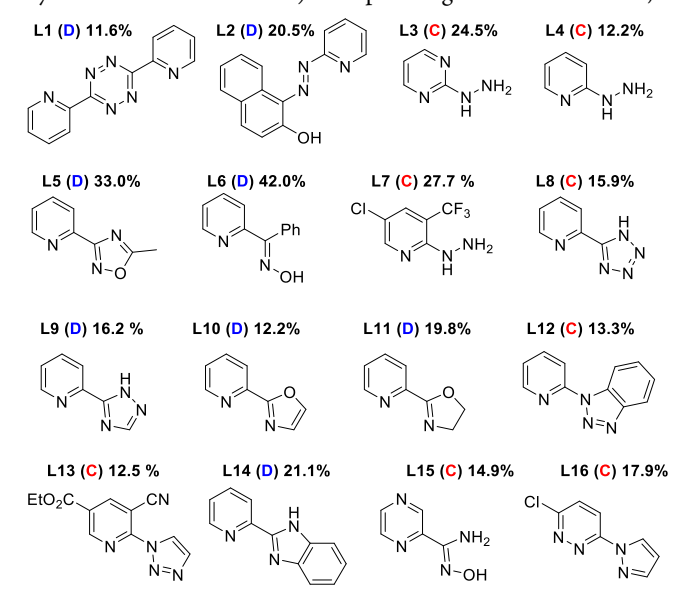
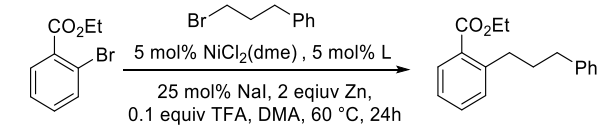


Figure 5. New ligand set B chosen intuitively using trend derived from the set T. Set B divided in half based upon calculations into predicted higher-performing (D, 8 members) and lower-performing (C, 8 members) sets. Assay yields are provided.



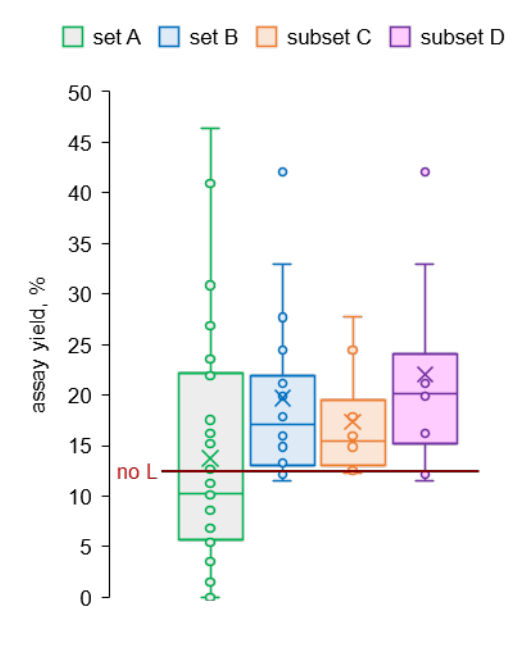


Figure 6. Distributions of assay yields for the depicted reaction for four specified ligand sets. Mean yield markers (\times) provided for every distribution. Medians are denoted by a bar and are inclusive. The red line across the graph defines a control, assay yield without a ligand (12.3%).

the median yield provided by set A is lower than a reaction run without a ligand. In contrast, set B—which was selected empirically based on the intial model—provided a higher median and mean yield, as well as a tighter distribution of yields. Notably, nearly any ligand from sets B–D provides higher yield than the ligandless control. These results demonstrate the advantage to generating an intial reactivity trend and using it to inform ligand selection.

The distribution of yields for subsets C and D demonstrate the benefits of an additional level of refinement in the empirically conceived ligand set. The proposed model (eq 1) dissects the set B in a qualitatively correct manner, despite its simplicity. Thus, the set comprised of ligands predicted to provide lower yield does have a lower mean and median yield relative to a parent set B. Similarly, ligands that were predicted to provide higher reactivity, do provide higher mean and median yields. Addition of a quantitative factor in the empirical library design process had a net positive effect, shifting yield distribution towards higher values. The difference between yield distributions observed for sets D and A highlights the efficiency of this combined ligand discovery approach relative to a conventional non-directed screening. For set D, mean and median yields are almost double those in set A, with a higher overall hit-rate.

New Ligands. Having interrogated the general yield distribution characteristics of sets A–D, we further investigated the constituents of set B. We evaluated ligands L1–16 in the XEC of a variety of (hetero)aryl bromides (**S1–S9**). Their performance compared to a selection of PyCam ligands (**E1-E7**) is reported in Figure 7. While generally high performing, the two best new ligands, **L5** and **L6** (members of the subset D), were relatively inefficient in

coupling substrates that do not have *ortho*-coordinating groups (**S5** and **S7**). This bias is consistent with the test reaction chosen and highlights the importance of the reaction used to search for ligands. We have previously found "cryptic ligands" that are general, but only for substrate combinations less commonly employed in academia.³⁷ As the *ortho*-coordination group of the substrate is changed from the original case (**S2** to **S3**) and then disappears altogether (to **S5** and **S7**), the performance of **L5** and **L6** decreases. However, **L5** and **L6** demonstrated promising reactivity in coupling of pharmaceutically-relevant pyrazole **S6**, quinoline **S8**, and benzimidazole **S9** cores. In all three cases, ligands **L5** and **L6** perform similarly to or even outperform the best PyCam ligands (**E1** and **E2**).

These promising results prompted further exploration of variants of L6 (that we refer to as PyOximes) in couplings of various α -haloazines (Figure 8, **S8-S12**). We focused on ligand **L6** instead of L5 for ease of access to derivatives. We compared the reactivity of these new ligands (PyOxime-1 to PyOxime-7) against multiple controls (E1 and E2, and bpy-based ligands). For every reaction tested, the pyridine-oxime ligands outperformed the control ligands (Figure 8). We also investigated PyOximes 2-7 to determine what structural features are critical to the observed reactivity. First, a free hydroxy group is not a critical functionality (PyOxime-7 performs well). Second, steric effects may be important: tert-butyl substituted ligand PyOxime-5 performed worse than PyOxime-4 and PyOximes-6. Finally, it appears that more electron rich PyOximes are not as efficient as corresponding electron-poor analogues (compare PyOxime-3 to PyOximes-1 and -2), consistent with the initially observed relation (vide supra).

	Ligands From Set B (Figure 5)														PyCam Ligands							1		
	L1	L2	L3	L4	L5	L6	L7	L8	L9	L10	L11	L12	L13	L14	L15	L16	E1	E2	E3	E4	E5	E6	E7	No L
S1	0.8	1.3	1.6	1.2	1.5	1.8	1.6	1.0	1.3	1.1	0.7	1.1	0.9	1.3	1.3	1.5	1.8	0.6	1.4	1.1	1.7	1.1	1.3	1.2
S2	0.8	1.4	1.7	0.9	2.3	3.0	2.0	1.1	1.1	0.9	1.4	0.9	0.9	1.5	1.1	1.3	3.0	0.8	2.6	0.6	2.0	0.7	1.7	0.6
S3	0.6	0.7	0.9	1.1	0.7	0.5	0.9	0.8	0.7	0.9	0.7	0.7	0.6	0.9	0.5	0.9	1.4	0.7	0.9	0.9	0.8	0.8	1.0	0.9
S4	1.0	-	0.8	-	1.0	1.2	0.7	0.9	1.0	0.7	0.4	0.5	0.7	0.7	1.2	1.1	1.4	0.9	0.8	-	1.1	0.8	1.2	-
S 5	0.5	0.0	0.0	0.0	0.2	0.2	0.0	0.1	0.5	0.0	0.0	0.0	0.1	0.3	0.1	0.2	0.9	0.9	0.3	0.0	0.4	0.0	0.5	0.0
S6	0.0	0.0	0.0	0.0	0.2	0.1	0.0	0.0	0.1	0.0	0.0	-	0.0	0.0	0.0	0.0	0.0	0.0	0.1	0.0	0.0	0.0	0.0	0.0
S 7	0.1	0.0	0.1	0.1	0.5	0.2	0.0	0.2	0.3	0.1	0.1	0.0	0.0	0.3	0.0	0.3	0.7	1.0	0.5	0.0	-	0.0	0.2	0.0
S8	1.0	0.7	0.0	0.0	0.4	0.7	0.0	0.5	0.3	0.1	0.0	0.2	0.4	0.1	0.2	0.3	0.2	0.5	0.2	0.0	0.1	0.0	0.2	0.0
S9	0.1	0.3	0.3	0.2	0.6	0.6	0.3	0.2	0.2	0.3	0.3	0.1	0.1	0.2	0.1	0.3	0.6	0.3	0.3	0.3	0.2	0.3	0.3	0.3

Figure 7. High-throughput exploration of ligand and substrate spaces. Reactions performed on 20 μ mol scale, in duplicates. Average product-to-standard (P/S) ratios are provided for each ligand-substrate combination. Each row is independently color-coded, with darker shades of green indicating higher P/S ratio.

(B) HTS testing of novel ligand framework

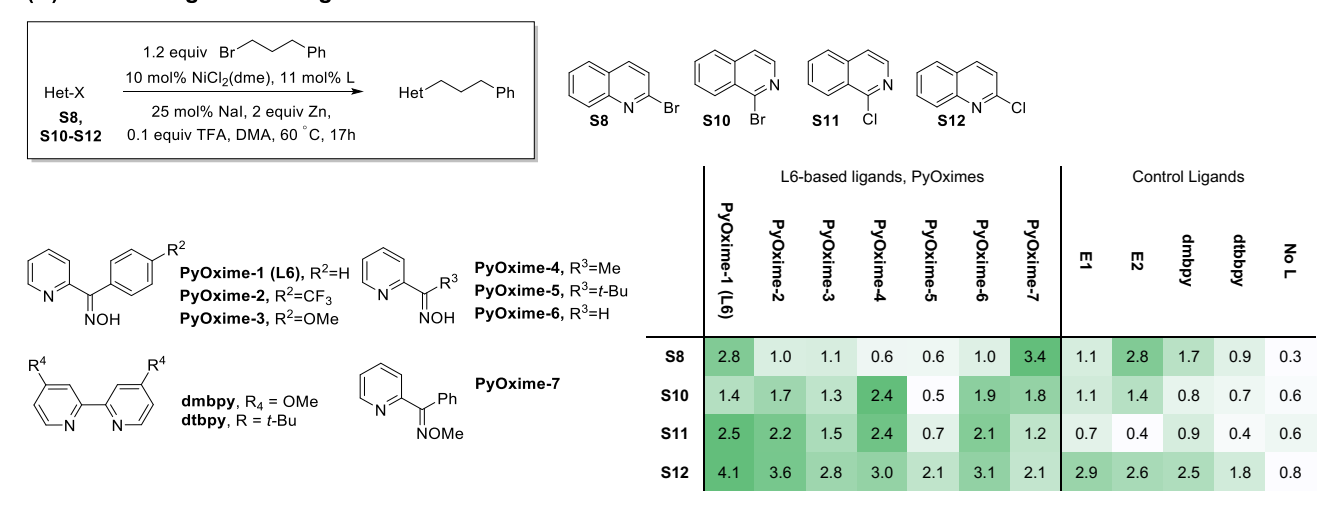


Figure 8. High-throughput exploration of ligand and substrate spaces. Reactions performed on 20 μ mol scale, in duplicates. Average product-to-standard (P/S) ratios are provided for each ligand-substrate combination. Each row is independently color-coded, with darker shades of green indicating higher P/S ratio.

We then analyzed absolute ligand performance for couplings of quinoline and isoquinoline electrophiles (Figure 9) on a typical synthetic scale (100 mg). In all four cases, pyridine-oxime ligands outperformed the best PyCam ligands, with synthetically useful yields obtained for important quinoline and isoquinoline substrates. Pyridyl oxadiazole ligand **L5** performed better than **E2** with isoquinolines, but was not as uniformly superior in this substrate class. To the best of our knowledge, these are some of the highest yields for $C(sp^2)-C(sp^3)$ XEC reactions reported for 2-halo azines under similar conditions. We could find only a single example of the coupling of S8 with an alkyl *N*-hydroxyphthalimide ester using 20 mol% nickel and no examples of couplings with S10-S12.⁴⁰⁻⁴²

Figure 9. Assay yields observed with pyridine-oxime and PyCam-based catalytic systems in couplings of various electrophiles. Assay yields were determined using UPLC against 2,2'-dimethylbiphenyl as internal standard. Yields labeled with asterisk were obtained using 5 mol% Ni.

Mechanistic Study. To the best of our knowledge, **L6** has never been used as a ligand in Ni-catalyzed XEC. Naturally, the question of the origin of the impressive performance of the **L6**-based catalysts arose. Given the prevalence of imine and amidine ligands, we were interested in establishing whether the N-O bond is stable under reaction conditions. Additionally, we wanted to understand if the reactivity in **L6**-based systems can be attributed to a specific portion of a catalytic cycle.

While pyridine oximes have not been utilized in XEC chemistry, their coordination chemistry has been extensively studied. 43,44 Complexes of Co(II)/Co(III),⁴⁵ Rh(III) and Ir(III)⁴⁶, Cu(II)⁴⁷ have been described, as well as a variety of Ni complexes. 48,49 In all of these complexes, the N-O bond of the oxime moiety remains intact, and the ligand typically binds to the transition metal via both available nitrogen atoms. Oxidative addition of the oxime N-O bond takes place only with very electron rich metal centers and activated oximes.50-53 There is evidence to suggest that even phosphinesupported Ni(0) is not a strong enough reductant to readily cleave N-O bonds in unactivated aldoximes. 54 Similarly, free ketoximes do not undergo N-O cleavage, even under harsh reaction conditions.⁵⁵ In agreement with these reports, our control experiments demonstrated complete stability of the oxime in the presence of Ni(II) and only partial ligand decomposition under forcing conditions with Ni(0) (See SI). On the basis of these results, we theorize that the efficiency of L6 can be mainly attributed to traditional N,N-bound complexes.

Our initial computational investigation did not find large differences in the calculated barriers for oxidative addition, radical association, and reductive elimination steps for bpy and L6 systems (see SI). Therefore, we expect that the relative efficiency of **L6** can be attributed to facile post-reductive elimination regeneration of the active Ni catalyst and/or supression of undesired reactions that we did not study in detail (e.g., aryl dimerization). Indeed, the computed relative redox potentials indicate that reduction of (L)NiBr₂ to (L)Ni, and oxidation of (L)NiBr to (L)NiBr₂ are more favorable for the PyOxime than for the bpy-supported Ni (see SI for details). Additionally, calculations suggest that oxidative addition of Ar-Br to (L)NiAr to form (L)NiAr2Br is less favorable for the PyOxime-ligated complex compared to the bpy analogue, which could minimize undesired aryl dimerization. In general, computationally assesed redox behavior of the oxime-supported Ni complex is in line with the nature of the identified statistical model (eq 1): PyOxime-bound complexes are more electron-poor then bpy complexes.

Conclusions

These results demonstrate that even simple computational models can increase the efficiency of ligand discovery from large libraries of compounds compared to undirected screening. The lower cost of this combined method (involving relatively simple computations and smaller ligand screens) increases accessibility. Our application of this approach to nickel-catalyzed cross-electrophile coupling demonstrates the promise of this approach by finding two new classes of ligands. The newly discovered ligands, particularly PyOximes, show promising performance in the XEC of 2-halo heterocyclic electrophiles. At Pfizer, PyOximes have demonstrated performance superior to all other tested ligands in couplings of haloazines on multiple occasions. Further studies on ligands L5 and L6, as well as the development of a more general understanding of nitrogen-based ligand reactivity will be reported in due course.

ASSOCIATED CONTENT

Supporting Information. Experimental procedures, characterization data and computational details provided in a supporting Information section. These materials available free of charge via the Internet at http://pubs.acs.org.

AUTHOR INFORMATION

Corresponding Author

* E-mail: dweix@wisc.edu, sebastien.monfette@pfizer.com and eric.hansen@pfizer.com

Funding Sources

This work was supported by the NSF (CHE-1900366).

ACKNOWLEDGMENT

Thanks goes to Dr. Joel Hawkins, Dr. Thomas Knauber, Dr. Russel Algera and Dr. Shu Yu (Pfizer) for helpful and stimulating discussions. Mr. Brian Jones (Pfizer) is acknowledged for obtaining accurate mass spec data. Authors are grateful to Sigma-Aldrich for providing assistance in the synthesis of ligands **PyOxime-2-7**. Authors thank the participants in the Pharma Alliance at AbbVie, Pfizer and Boehringer Ingelheim for their helpful discussions.

REFERENCES

- (1) Engle, K. M.; Yu, J.-Q. Developing Ligands for Palladium(II)-Catalyzed C-H Functionalization: Intimate Dialogue between Ligand and Substrate. J. Org. Chem. 2013, 78 (18), 8927–8955. https://doi.org/10.1021/jo400159y.
- (2) Vogiatzis, K. D.; Polynski, M. V; Kirkland, J. K.; Townsend, J.; Hashemi, A.; Liu, C.; Pidko, E. A. Computational Approach to Molecular Catalysis by 3d Transition Metals: Challenges and Opportunities. Chem. Rev. 2019, 119 (4), 2453–2523. https://doi.org/10.1021/acs.chemrev.8b00361.
- (3) Poree, C.; Schoenebeck, F. A Holy Grail in Chemistry: Computational Catalyst Design: Feasible or Fiction? *Acc. Chem. Res.* **2017**, *50* (3), 605–608. https://doi.org/10.1021/acs.accounts.6b00606.
- (4) Gensch, T.; dos Passos Gomes, G.; Friederich, P.; Peters, E.; Gaudin, T.; Pollice, R.; Jorner, K.; Nigam, A.; Lindner-D'Addario, M.; Sigman, M. S.; Aspuru-Guzik, A. A Comprehensive Discovery Platform for Organophosphorus Ligands for Catalysis. J. Am. Chem. Soc. 2022, 144 (3), 1205–1217. https://doi.org/10.1021/jacs.1c09718.
- (5) Xu, J.; Grosslight, S.; Mack, K. A.; Nguyen, S. C.; Clagg, K.; Lim, N.-K.; Timmerman, J. C.; Shen, J.; White, N. A.; Sirois, L. E.; Han, C.; Zhang, H.; Sigman, M. S.; Gosselin, F. Atroposelective Negishi Coupling Optimization Guided by Multivariate Linear Regression Analysis: Asymmetric Synthesis of KRAS G12C Covalent Inhibitor

- GDC-6036. J. Am. Chem. Soc. **2022**, 144 (45), 20955–20963. https://doi.org/10.1021/jacs.2c09917.
- (6) Robinson, S. G.; Wu, X.; Jiang, B.; Sigman, M. S.; Lin, S. Mechanistic Studies Inform Design of Improved Ti(Salen) Catalysts for Enantioselective [3 + 2] Cycloaddition. J. Am. Chem. Soc. 2020, 142 (43), 18471–18482. https://doi.org/10.1021/jacs.0c07128.
- (7) Liles, J. P.; Rouget-Virbel, C.; Wahlman, J. L. H.; Rahimoff, R.; Crawford, J. M.; Medlin, A.; O'Connor, V. S.; Li, J.; Roytman, V. A.; Toste, F. D.; Sigman, M. S. Data Science Enables the Development of a New Class of Chiral Phosphoric Acid Catalysts. *Chem* 2023, 9 (6), 1518–1537.
- https://doi.org/https://doi.org/10.1016/j.chempr.2023.02.020.

 (8) Laffoon, S. D.; Chan, V. S.; Fickes, M. G.; Kotecki, B.; Ickes, A. R.; Henle, J.; Napolitano, J. G.; Franczyk, T. S.; Dunn, T. B.; Barnes, D. M.; Haight, A. R.; Henry, R. F.; Shekhar, S. Pd-Catalyzed Cross-Coupling Reactions Promoted by Biaryl Phosphorinane Ligands. ACS Catal. 2019, 9 (12), 11691–11708. https://doi.org/10.1021/acscatal.9b03012.
- (9) Chen, Y.-Q.; Wang, Z.; Wu, Y.; Wisniewski, S. R.; Qiao, J. X.; Ewing, W. R.; Eastgate, M. D.; Yu, J.-Q. Overcoming the Limitations of γ- and δ-C–H Arylation of Amines through Ligand Development. J. Am. Chem. Soc. 2018, 140 (51), 17884–17894. https://doi.org/10.1021/jacs.8b07109.
- (10) Jones, D. J.; Gibson, V. C.; Green, S. M.; Maddox, P. J.; White, A. J. P.; Williams, D. J. Discovery and Optimization of New Chromium Catalysts for Ethylene Oligomerization and Polymerization Aided by High-Throughput Screening. J. Am. Chem. Soc. 2005, 127 (31), 11037–11046. https://doi.org/10.1021/ja0518171.
- (11) McNally, A.; Prier, C. K.; MacMillan, D. W. C. Discovery of an α-Amino C–H Arylation Reaction Using the Strategy of Accelerated Serendipity. Science (80-.). 2011, 334 (6059), 1114–1117. https://doi.org/10.1126/science.1213920.
- (12) Isbrandt, E. S.; Sullivan, R. J.; Newman, S. G. High Throughput Strategies for the Discovery and Optimization of Catalytic Reactions. Angew. Chemie Int. Ed. 2019, 58 (22), 7180–7191. https://doi.org/10.1002/anie.201812534.
- (13) Collins, K. D.; Gensch, T.; Glorius, F. Contemporary Screening Approaches to Reaction Discovery and Development. *Nat. Chem.* 2014, 6 (10), 859–871. https://doi.org/10.1038/nchem.2062.
- (14) Mennen, S. M.; Alhambra, C.; Allen, C. L.; Barberis, M.; Berritt, S.; Brandt, T. A.; Campbell, A. D.; Castañón, J.; Cherney, A. H.; Christensen, M.; Damon, D. B.; Eugenio de Diego, J.; García-Cerrada, S.; García-Losada, P.; Haro, R.; Janey, J.; Leitch, D. C.; Li, L.; Liu, F.; Lobben, P. C.; MacMillan, D. W. C.; Magano, J.; McInturff, E.; Monfette, S.; Post, R. J.; Schultz, D.; Sitter, B. J.; Stevens, J. M.; Strambeanu, I. I.; Twilton, J.; Wang, K.; Zajac, M. A. The Evolution of High-Throughput Experimentation in Pharmaceutical Development and Perspectives on the Future. Org. Process Res. Dev. 2019, 23 (6), 1213–1242. https://doi.org/10.1021/acs.oprd.9b00140.
- (15) Hansen, E. C.; Pedro, D. J.; Wotal, A. C.; Gower, N. J.; Nelson, J. D.; Caron, S.; Weix, D. J. New Ligands for Nickel Catalysis from Diverse Pharmaceutical Heterocycle Libraries. *Nat. Chem.* 2016, 8 (12), 1126–1130. https://doi.org/10.1038/nchem.2587.
- (16) Hansen, E. C.; Li, C.; Yang, S.; Pedro, D.; Weix, D. J. Coupling of Challenging Heteroaryl Halides with Alkyl Halides via Nickel-Catalyzed Cross-Electrophile Coupling. J. Org. Chem. 2017, 82 (14), 7085–7092. https://doi.org/10.1021/acs.joc.7b01334.
- (17) Fu, J.; Lundy, W.; Chowdhury, R.; Twitty, J. C.; Dinh, L. P.; Sampson, J.; Lam, Y.; Sevov, C. S.; Watson, M. P.; Kalyani, D. Nickel-Catalyzed Electroreductive Coupling of Alkylpyridinium Salts and Aryl Halides. ACS Catal. 2023, 13 (14), 9336–9345. https://doi.org/10.1021/acscatal.3c01939.
- (18) Biswas, S.; Qu, B.; Desrosiers, J.-N.; Choi, Y.; Haddad, N.; Yee, N. K.; Song, J. J.; Senanayake, C. H. Nickel-Catalyzed Cross-Electrophile Reductive Couplings of Neopentyl Bromides with Aryl Bromides. J. Org. Chem. 2020, 85 (12), 8214–8220. https://doi.org/10.1021/acs.joc.0c00549.
- (19) Modak, A.; Nett, A. J.; Swift, E. C.; Haibach, M. C.; Chan, V. S.; Franczyk, T. S.; Shekhar, S.; Cook, S. P. Cu-Catalyzed C–N Coupling with Sterically Hindered Partners. ACS Catal. 2020, 10 (18), 10495–

- 10499. https://doi.org/10.1021/acscatal.0c02965.
- (20) Prieto Kullmer, C. N.; Kautzky, J. A.; Krska, S. W.; Nowak, T.; Dreher, S. D.; MacMillan, D. W. C. Accelerating Reaction Generality and Mechanistic Insight through Additive Mapping. Science (80-.). 2022, 376 (6592), 532–539. https://doi.org/10.1126/science.abn1885.
- (21) Ahn, S.; Hong, M.; Sundararajan, M.; Ess, D. H.; Baik, M.-H. Design and Optimization of Catalysts Based on Mechanistic Insights Derived from Quantum Chemical Reaction Modeling. *Chem. Rev.* 2019, 119 (11), 6509–6560. https://doi.org/10.1021/acs.chemrev.9b00073.
- (22) Hopkinson, M. N.; Gómez-Suárez, A.; Teders, M.; Sahoo, B.; Glorius, F. Accelerated Discovery in Photocatalysis Using a Mechanism-Based Screening Method. Angew. Chemie Int. Ed. 2016, 55 (13), 4361–4366. https://doi.org/10.1002/anie.201600995.
- (23) Durand, D. J.; Fey, N. Computational Ligand Descriptors for Catalyst Design. *Chem. Rev.* **2019**, 119 (11), 6561–6594. https://doi.org/10.1021/acs.chemrev.8b00588.
- (24) Ahneman, D. T.; Estrada, J. G.; Lin, S.; Dreher, S. D.; Doyle, A. G. Predicting Reaction Performance in C–N Cross-Coupling Using Machine Learning. *Science* (80-.). 2018, 360 (6385), 186 LP 190. https://doi.org/10.1126/science.aar5169.
- (25) Zhao, S.; Gensch, T.; Murray, B.; Niemeyer, Z. L.; Sigman, M. S.; Biscoe, M. R. Enantiodivergent Pd-Catalyzed C–C Bond Formation Enabled through Ligand Parameterization. *Science* (80-.). 2018, 362 (6415), 670 LP – 674. https://doi.org/10.1126/science.aat2299.
- (26) Kim, S.; Goldfogel, M. J.; Gilbert, M. M.; Weix, D. J. Nickel-Catalyzed Cross-Electrophile Coupling of Aryl Chlorides with Primary Alkyl Chlorides. J. Am. Chem. Soc. 2020, 142 (22), 9902–9907. https://doi.org/10.1021/jacs.0c02673.
- (27) Perkins, R. J.; Hughes, A. J.; Weix, D. J.; Hansen, E. C. Metal-Reductant-Free Electrochemical Nickel-Catalyzed Couplings of Aryl and Alkyl Bromides in Acetonitrile. Org. Process Res. Dev. 2019, 23 (8), 1746–1751. https://doi.org/10.1021/acs.oprd.9b00232.
- (28) Anka-Lufford, L. L.; Huihui, K. M. M.; Gower, N. J.; Ackerman, L. K. G.; Weix, D. J. Nickel-Catalyzed Cross-Electrophile Coupling with Organic Reductants in Non-Amide Solvents. Chem. A Eur. J. 2016, 22 (33), 11564–11567. https://doi.org/10.1002/chem.201602668.
- (29) Weix, D. J. Methods and Mechanisms for Cross-Electrophile Coupling of Csp2 Halides with Alkyl Electrophiles. Acc. Chem. Res. 2015, 48 (6), 1767–1775. https://doi.org/10.1021/acs.accounts.5b00057.
- (30) Everson, D. A.; Shrestha, R.; Weix, D. J. Nickel-Catalyzed Reductive Cross-Coupling of Aryl Halides with Alkyl Halides. J. Am. Chem. Soc. 2010, 132 (3), 920–921. https://doi.org/10.1021/ja9093956.
- (31) Yu, X.; Yang, T.; Wang, S.; Xu, H.; Gong, H. Nickel-Catalyzed Reductive Cross-Coupling of Unactivated Alkyl Halides. Org. Lett. 2011, 13 (8), 2138–2141. https://doi.org/10.1021/ol200617f.
- (32) Wang, S.; Qian, Q.; Gong, H. Nickel-Catalyzed Reductive Coupling of Aryl Halides with Secondary Alkyl Bromides and Allylic Acetate. *Org. Lett.* **2012**, 14 (13), 3352–3355. https://doi.org/10.1021/ol3013342.
- (33) Cherney, A. H.; Reisman, S. E. Nickel-Catalyzed Asymmetric Reductive Cross-Coupling Between Vinyl and Benzyl Electrophiles. *J. Am. Chem. Soc.* **2014**, 136 (41), 14365–14368. https://doi.org/10.1021/ja508067c.
- (34) Kadunce, N. T.; Reisman, S. E. Nickel-Catalyzed Asymmetric Reductive Cross-Coupling between Heteroaryl Iodides and α-Chloronitriles. *J. Am. Chem. Soc.* **2015**, *137* (33), 10480–10483. https://doi.org/10.1021/jacs.5b06466.
- (35) Wang, X.; Dai, Y.; Gong, H. Nickel-Catalyzed Reductive Couplings. Top. Curr. Chem. 2016, 374 (4), 43. https://doi.org/10.1007/s41061-016-0042-2.
- (36) Diccianni, J. B.; Diao, T. Mechanisms of Nickel-Catalyzed Cross-Coupling Reactions. Trends Chem. 2019, 1 (9), 830–844. https://doi.org/https://doi.org/10.1016/j.trechm.2019.08.004.
- (37) Aguirre, A. L.; Loud, N. L.; Johnson, K. A.; Weix, D. J.; Wang, Y. ChemBead Enabled High-Throughput Cross-Electrophile Coupling Reveals a New Complementary Ligand. Chem. A Eur. J. 2021, 27 (51), 12981–12986. https://doi.org/https://doi.org/10.1002/chem.202102347.
- (38) Biswas, S.; Weix, D. J. Mechanism and Selectivity in Nickel-Catalyzed Cross-Electrophile Coupling of Aryl Halides with Alkyl Halides. J. Am.

- Chem. Soc. **2013**, 135 (43), 16192–16197. https://doi.org/10.1021/ja407589e.
- (39) Lin, Q.; Diao, T. Mechanism of Ni-Catalyzed Reductive 1,2-Dicarbofunctionalization of Alkenes. J. Am. Chem. Soc. 2019, 141 (44), 17937–17948. https://doi.org/10.1021/jacs.9b10026.
- (40) Charboneau, D. J.; Barth, E. L.; Hazari, N.; Uehling, M. R.; Zultanski, S. L. A Widely Applicable Dual Catalytic System for Cross-Electrophile Coupling Enabled by Mechanistic Studies. ACS Catal. 2020, 10 (21), 12642–12656. https://doi.org/10.1021/acscatal.0c03237.
- (41) DeCicco, E. M.; Berritt, S.; Knauber, T.; Coffey, S. B.; Hou, J.; Dowling, M. S. Decarboxylative Cross-Electrophile Coupling of (Hetero)Aromatic Bromides and NHP Esters. J. Org. Chem. 2023, 88 (17), 12329–12340. https://doi.org/10.1021/acs.joc.3c01072.
- (42) Molander, G. A.; Traister, K. M.; O'Neill, B. T. Reductive Cross-Coupling of Nonaromatic, Heterocyclic Bromides with Aryl and Heteroaryl Bromides. J. Org. Chem. 2014, 79 (12), 5771–5780. https://doi.org/10.1021/jo500905m.
- (43) Kukushkin, V. Y.; Pombeiro, A. J. L. Oxime and Oximate Metal Complexes: Unconventional Synthesis and Reactivity. Coord. Chem. Rev. 1999, 181 (1), 147–175. https://doi.org/https://doi.org/10.1016/S0010-8545(98)00215-X.
- (44) Milios, C. J.; Stamatatos, T. C.; Perlepes, S. P. The Coordination Chemistry of Pyridyl Oximes. *Polyhedron* 2006, 25 (1), 134–194. https://doi.org/https://doi.org/10.1016/j.poly.2005.07.022.
- (45) Stamatatos, T. C.; Bell, A.; Cooper, P.; Terzis, A.; Raptopoulou, C. P.; Heath, S. L.; Winpenny, R. E. P.; Perlepes, S. P. Old Ligands with New Coordination Chemistry: Linear Trinuclear Mixed Oxidation State Cobalt(III/IIII) Complexes and Their Mononuclear "Ligand" Cobalt(III) Complexes Featuring 2-Pyridyloximates. Inorg. Chem. Commun. 2005, 8 (6), 533–538. https://doi.org/https://doi.org/10.1016/j.inoche.2005.03.004.
- (46) Adhikari, S.; Palepu, N. R.; Sutradhar, D.; Shepherd, S. L.; Phillips, R. M.; Kaminsky, W.; Chandra, A. K.; Kollipara, M. R. Neutral and Cationic Half-Sandwich Arene Ruthenium, Cp*Rh and Cp*Ir Oximato and Oxime Complexes: Synthesis, Structural, DFT and Biological Studies. J. Organomet. Chem. 2016, 820, 70–81. https://doi.org/https://doi.org/10.1016/j.jorganchem.2016.08.004
- (47) Li, R.; Lu, J.; Li, D.; Cheng, S.; Dou, J. Syntheses, Structures, in Vitro Cytotoxicities and DNA-Binding Properties of Four Copper Complexes Based on a Phenyl 2-Pyridyl Ketoxime Ligand. *Transit. Met. Chem.* 2014, 39 (5), 507–517. https://doi.org/10.1007/s11243-014-9826-9
- (48) Papatriantafyllopoulou, C.; Aromi, G.; Tasiopoulos, A. J.; Nastopoulos, V.; Raptopoulou, C. P.; Teat, S. J.; Escuer, A.; Perlepes, S. P. Use of the Sulfato Ligand in 3d-Metal Cluster Chemistry: A Family of Hexanuclear Nickel(II) Complexes with 2-Pyridyl-Substituted Oxime Ligands. Eur. J. Inorg. Chem. 2007, 2007 (18), 2761–2774. https://doi.org/https://doi.org/10.1002/ejic.200700063.
- (49) Chaudhuri, P.; Weyhermüller, T.; Wagner, R.; Khanra, S.; Biswas, B.; Bothe, E.; Bill, E. Tridentate Facial Ligation of Tris(Pyridine-2-Aldoximato)Nickel(II) and Tris(Imidazole-2-Aldoximato)Nickel(II) To Generate NiIIFeIIINiII, MnIIINiII, NiIINiII, and ZnIINiIII and the Electrooxidized MnIVNiII, NiIINiIII, and ZnIINiIII Species: A Magnetostruc. Inorg. Chem. 2007, 46 (21), 9003–9016.
- (50) Kitamura, M.; Narasaka, K. Synthesis of Aza-Heterocycles from Oximes by Amino-Heck Reaction. Chem. Rec. 2002, 2 (4), 268–277. https://doi.org/https://doi.org/10.1002/tcr.10030.

https://doi.org/10.1021/ic701073j.

- (51) Tan, Y.; Hartwig, J. F. Palladium-Catalyzed Amination of Aromatic C–H Bonds with Oxime Esters. J. Am. Chem. Soc. 2010, 132 (11), 3676–3677. https://doi.org/10.1021/ja100676r.
- (52) M. P. Ferreira, C.; Fátima C. Guedes da Silva, M.; Yu. Kukushkin, V.; J. R. Fraústo da Silva, J.; J. L. Pombeiro, A. The First Direct Observation of N-O Bond Cleavage in the Oxidative Addition of an Oxime to a Metal Centre. Synthesis and Crystal Structure of the Methyleneamide Complex Trans-

- [Re(OH)(N\(\text{DCMe2}\))(Ph2PCH2CH2PPh2)2][HSO4]. *J. Chem. Soc. Dalt.* Trans. 1998, No. 3, 325–326. https://doi.org/10.1039/A707213I.
- (53) Bogdos, M. K.; Müller, P.; Morandi, B. Structural Evidence for Aromatic Heterocycle N-O Bond Activation via Oxidative Addition. Organometallics 2023, 42 (3), 211–217. https://doi.org/10.1021/acs.organomet.2c00533.
- (54) Takahashi, Y.; Tsuji, H.; Kawatsura, M. Nickel-Catalyzed Transformation of Alkene-Tethered Oxime Ethers to Nitriles by a Traceless Directing Group Strategy. J. Org. Chem. 2020, 85 (4), 2654– 2665. https://doi.org/10.1021/acs.joc.9b02705.
- Yoshida, Y.; Kurahashi, T.; Matsubara, S. Nickel-Catalyzed Cycloaddition of Aromatic (O-Benzyl)Ketoximes with Alkynes to Produce Isoquinoline and Isoquinoline N-Oxide Derivatives. Chem. Lett. 2011, 40 (10), 1140–1142. https://doi.org/10.1246/cl.2011.1140.

TOC Graphic

Computationally guided ligand discovery: screening, chemical intuition, and modeling

